Acta Polytechnica CTU Proceedings **42**:1–5, 2023
https://doi.org/10.14311/APP.2023.42.0001

Published by the Czech Technical University in Prague

EFFECT OF AGING ON MECHANICAL PROPERTIES OF 3D PRINTED SAMPLES USING STEREOLITOGRAPHY

Veronika Drechslerová[a,*], Jan Falta[a], Tomáš Fíla[a], Radim Dvořák[a], Daniel Kytýř[b]

[a] *Czech Technical University in Prague, Faculty of Transportation Sciences, Department of Mechanics and Materials, Na Florenci 25, 110 00 Prague 1, Czech Republic*

[b] *Czech Academy of Sciences, Institute of Theoretical and Applied Mechanics, Prosecká, 809/76, 190 00 Prague 9, Czech Republic*

[*] corresponding author: drechver@fd.cvut.cz

Abstract. This paper focuses on stereolithography (an additive manufacturing technology working on the principle of curing liquid resins layer by layer using ultraviolet radiation) and the effect of aging on the mechanical properties of the material and printed samples. The aging of the material could be a problem for its subsequent use as the stability of the mechanical properties would not be maintained and unwanted deterioration of the material could occur. As part of the research, sets of samples were printed and subjected to different aging methods and subsequently subjected to quasi-static and dynamic uni-axial load tests. From the data obtained, the basic mechanical properties of the material were calculated and compared with each other. The aim of this paper was to investigate whether aging process causes significant changes in the mechanical properties of the materials used, which could have a consequential impact on their use in different industries.

Keywords: Stereolithography, aging, mechanical properties, quasi-static testing, dynamic testing.

1. Introduction

The rapid advancement of additive manufacturing technologies has revolutionized the production of complex and customized parts. Stereolithography, a popular additive manufacturing technique, utilizes the principle of curing liquid resins layer by layer using ultraviolet radiation [1, 2]. Compared to other additive manufacturing methods such as fused filament fabrication, sheet lamination or binder jetting, stereolithography achieves higher print accuracy, the ability to create individual intricate details and the possibility to produce parts with different mechanical properties.

While stereolithography has gained significant attention for its versatility and applications, the influence of aging on the mechanical properties of printed material has been relatively limitedly investigated. Aging processes (sunlight, X-ray), such as exposure to environmental factors, temperature fluctuations, or long-term usage, can potentially affect the structural integrity of the material and its overall performance [3, 4]. In a previous study, signs of the effect of aging on mechanical properties have already been observed, but it was difficult to find information on this phenomenon because the manufacturer did not provide this type of information and the scientific community has only recently started to focus on this issue. Understanding the impact of aging on samples printed by stereolithography is crucial for evaluating the long-term reliability and usability of these materials in various industrial sectors [5].

In this study, we investigate the effect of exposing printed samples by stereolithography to various aging effects and investigate their effect on the mechanical properties of the material and printed samples and on their behavior under loading. For this purpose, the aged samples were tested under quasi-static and dynamic uni-axial loading to evaluate their mechanical response.

2. Materials and methods

2.1. Materials

For manufacturing 3D samples the resin compatible (Aque Blue from Phrozen) with 3D printer Sonic Mighty 4K (Phrozen, Taiwan) was used. This resin was chosen based on previous research of Drechslerová 2023 [6] in which different resins and their mechanical properties were investigated. Among the resins analysed, Aque Blue resin achieved satisfactory values of mechanical properties and the samples printed from this material showed the required resistance to the tested loading. The chemical composition and more detailed information about the resin are given in the data sheet [7].

2.2. Sample preparation

Inventor Professional 2022 was used to design the test specimen models, and two types of test specimens were designed depending on the type of load test. For tensile loading, dog bone shape were designed. They were modeled based on the ASTM D638-14 standard. The basic proposed specimen dimensions are shown in Figure 1 and listed in Table 1. For easier

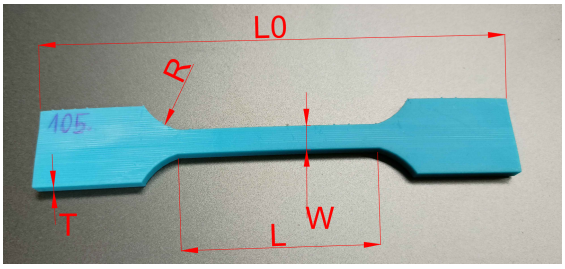

Figure 1. Basic dimensions of tensile sample used from ASTM D638-14 standard.

Parameter	Dim. [mm]
Thickness T	4
Gauge width W	6
Overall length L	115
Gauge length L_0	40
Curvature radius R	14

Table 1. Dimensions of the tensile test specimen.

manufacturing and to obtain higher quality of printed samples, the samples were printed rotated 60 ° about the x-axis and placed on supports.

For quasi-static and dynamic compressive loading, the bulk specimens were created. The design of the test specimens was based on the ASTM D695-15 standard, and the dimensions of the specimens were adapted to the loading devices. The basic proposed specimen dimensions are given in Table 2 and shown in Figure 2. To guarantee the quality of the 3D printed specimen, the specimens were rotated 40 ° rotation about the x and y-axes during manufacturing and placed on the supports (see Figure 3).

2.3. Samples post-treatment process

Test samples printed from resin require a post-treatment process to ensure that the final mechanical properties are achieved. As part of this process, the supports were removed, the samples were mechanically cleaned using spring water and chemically using isopropyl alcohol ultrasonic bath and then cured using a Cure Luna UV lamp (Phrozen, Taiwan). The specimens for tensile testing were cured for a total of one hour and the specimens for compressive loading were cured for 40 min. Halfway through the time, the cured specimens were inverted to ensure uniform irradiation, including the underside lying on the rotating platform of the UV lamp. Cure times were based on the manufacturer's recommendation of 30 min for the resin. To ensure complete curing to avoid subsequent degradation of mechanical properties, slightly higher times than those given by the manufacturer were chosen.

2.4. Aging methods

The samples were subjected to two types of aging, sunlight and extreme X-ray irradiation. To avoid exposing the samples to unwanted influences in the intervening

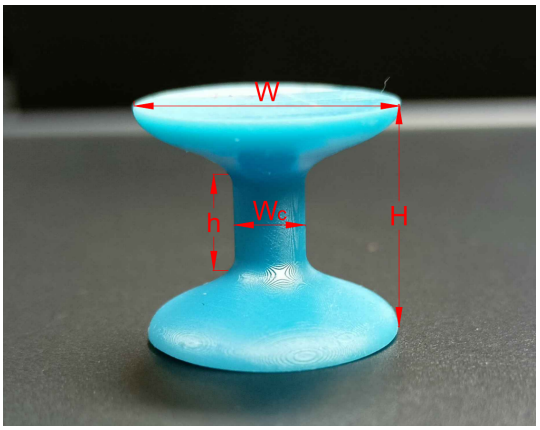

Figure 2. Basic dimensions of the sample for compression.

Parameter	Dim. [mm]
Base diameter W	18
Overall height H	16
Gauge diameter Wc	5
Gauge height h	8

Table 2. Dimensions of the compressive test specimen.

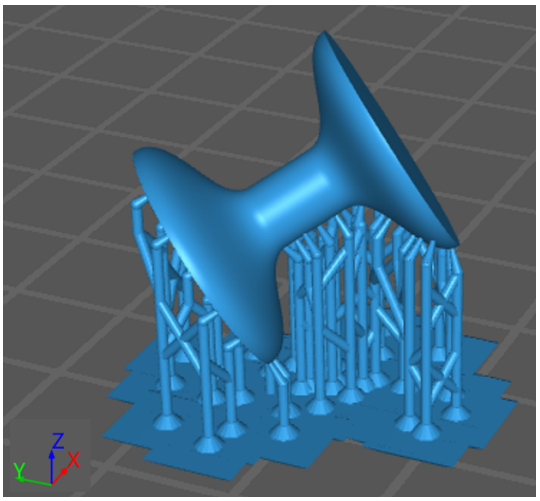

Figure 3. Rotated sample about the x and y-axes.

period between the completion of production and the application of the aging method under investigation, the samples were subjected to X-ray/sunlight immediately after removal from the UV lamp. The samples exposed to sunlight were placed between window panes to protect them from the weather conditions. The sets of samples were exposed to sunlight for 7 and 25 days during the month of May in Prague to compare the dependence of the effect of a given aging type on the exposure time. Using X-ray, the samples were placed one meter away from the radiation source and in the center of the radiation beam and irradiated for 1 and 2 h at 225 kV with radiation intensity of approx. 5000 R h^{-1}. The spread of the samples over a area

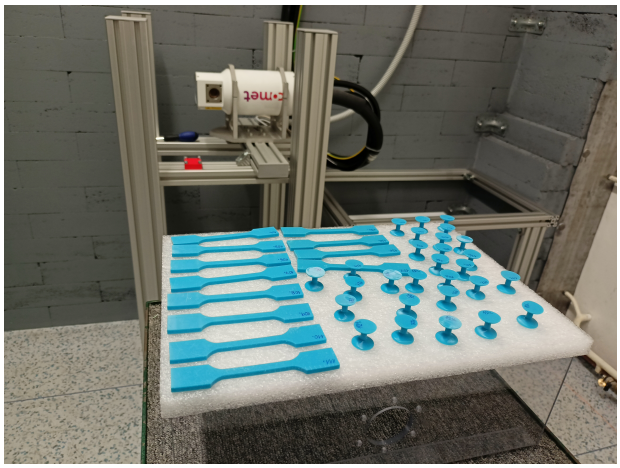

FIGURE 4. Printed samples subjected to X-ray.

(see Figure 4) did not affect the homogeneity of the radiation flux. To demonstrate the effect of aging on the mechanical properties of the material and printed samples, one set of samples was tested directly after production.

2.5. Experimental Procedure

In order to determine the basic mechanical properties and loading behavior, the printed samples were subjected to three types of loading:

- quasi-static tensile loading,
- quasi-static compressive loading,
- dynamic compressive loading.

Each set of test specimens contained 4 specimens, and a total of 20 tensile spesimens (4 sets – set for each aging effect and set of specimens tested immediately after production) and 40 bulk specimens (quasi-static and dynamic compressive testing) were tested. All specimens were measured and weighted before testing.

Quasi-static tensile testing was performed using an Instron 3382 (Instron Inc., USA) universal testing machine, in which the test specimens were subjected to the uni-axial tension. The loading rate was set at $3\,\mathrm{mm\,min^{-1}}$ according to ASTM D638-14 standard and the test was carried out until the specimen was broken. For the purpose of subsequent test evaluation and to obtain the basic mechanical properties, the dependence of the absolute elongation ΔL of the test specimen on the applied axial loading force F was recorded during testing. After the test, the length of the sample was remeasured.

The quasi-static compressive loading was performed on the same loading device as the tensile test. The loading rate was set at $1\,\mathrm{mm\,min^{-1}}$ and the test was terminated at the time of failure of the middle part of the specimen. During the test, as in the tensile test, the absolute change of the length of the test specimen ΔL was recorded depending on the applied axial loading force F.

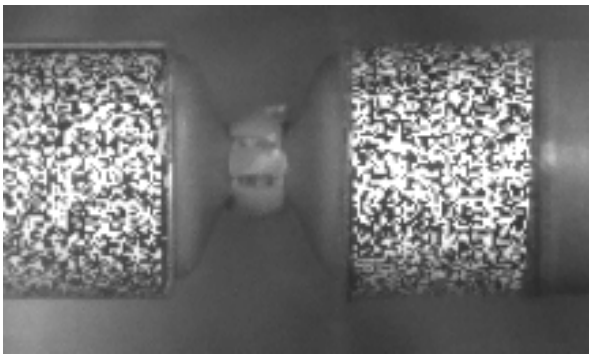

FIGURE 5. The disintegrating sample in Split Hopkinson Pressure Bar.

For dynamic compressive loading, the Split Hopkinson Pressure Bar (SHPB) was used (Figure 5) with the striker impact of velocity of $15\,\mathrm{m\,s^{-1}}$ [8]. Using the strain mounted on the bars, the required data was obtained for subsequent evaluation in order to obtain a more detailed description of the behaviour during loading.

2.6. Data Evaluation

All measured data from the load tests were evaluated in MATLAB (MathWorks, Inc., USA). To streamline the work, semi-automatic scripts were created and subsequently used to calculate the basic mechanical properties from quasi-static tensile loading and construct the stress-strain diagrams. The curves shown in the diagrams were obtained by averaging the individual specimens tested in a single set. The light broad line along each curve shows the scatter of the experimental values. For subsequent comparison, the obtained curves from each loading test were pasted into one stress-strain diagram. However, the data had to be adjusted (trimmed, smoothed, etc.) before the evaluation and calculation of the mechanical properties was performed.

The basic mechanical properties investigated were:

- Young's modulus of elasticity E in tension,
- yield stress $\sigma_{0.2}$ in tension,
- tensile strength σ_{U},
- ductility D.

The tensile strength σ_{U} and ductility D were determined from the measured dimensions of the test specimens before (the initial gauge length L_0 and the cross-sectional area parameter A_{C}) and after loading (the length of the specimen after breaking L_{u}). These measured values had to be entered manually into the generated semi-automatic scripts. The ductility D and the strain ϵ were calculated on the basis of the following relations

$$D = \frac{L_{\mathrm{u}} - L_0}{L_0} \cdot 100, \tag{1}$$

$$\epsilon = \frac{\triangle L}{L_0}. \tag{2}$$

Aging	Mechanical characteristic			
	E [MPa]	$\sigma_{0.2}$ [MPa]	σ_{U} [MPa]	ϵ_{tb} %
sunlight (0 days)	1500.66 ± 12.11	26.28 ± 0.85	38.40 ± 1.13	6.59 ± 1.46
sunlight (7 days)	2203.31 ± 32.44	37.60 ± 1.25	57.28 ± 0.47	1.39 ± 0.15
sunlight (25 days)	2108.38 ± 80.75	41.37 ± 1.88	57.08 ± 1.89	1.74 ± 0.25
X-ray (1 h)	1730.42 ± 76.49	32.97 ± 2.40	42.53 ± 2.80	3.43 ± 0.55
X-ray (2 h)	1669.45 ± 53.53	31.00 ± 1.31	41.76 ± 1.09	2.16 ± 0.35

Table 3. Tensile test mechanical characteristic values.

Furthermore, the tensile stresses σ_{T} and compressive stresses σ_{C} were calculated according to the following formulas

$$\sigma_{\mathrm{T}} = \frac{F}{A_{\mathrm{C}}} = \frac{F}{T \cdot W}, \tag{3}$$

$$\sigma_{\mathrm{C}} = \frac{F}{A_{\mathrm{C}}} = \frac{F}{\pi \cdot (0.5 \cdot W_{\mathrm{c}})^2}, \tag{4}$$

where T is the thickness, W is the gauge width and W_{c} is the gauge diameter of the tested specimen.

The Young's modulus of elasticity E in tension and the yield stress $\sigma_{0.2}$ in tension were obtained from auxiliary diagrams created within the script. The Young's modulus of elasticity E was defined as the ratio of stress to strain on the linear section of the tension curve.

3. Results

3.1. Quasi-static tensile loading

The basic mechanical properties of the material were calculated from the measured tensile test data. The data obtained from the individual measurements were averaged and the average values of the individual mechanical properties are given in Table 3. Furthermore, average curves of the individual aging effects were generated from the average stress and strain. These average curves were compared with each other and are presented in Figure 6.

From the results obtained in Table 3 it can be seen that highest values of deformation and stress were achieved by samples exposed to aging by sunlight, while the lowest values were achieved by samples tested immediately after manufacturing. Samples exposed to X-ray for 1 and 2 h show similarly high values of deformation and stress, while the values of samples irradiated for 2 h lie within the measurement uncertainty range for 1 h of exposure.

From a comparison of the curves representing the different effects of aging in the tensile diagram, it can be noticed that the curves corresponding to the samples exposed to solar radiation are almost identical, differing only by a different standard deviation. A similar trend can be observed for the X-ray exposed samples. It can also be observed from the curves that the samples exposed to sunlight show a greater strengthening of the material but an earlier failure compared to, for example, samples tested immediately after manufacture. It can also be seen that the trends of the curves of samples subjected to X-rays are similar, but that those subjected to X-rays for a longer period of time show earlier failure.

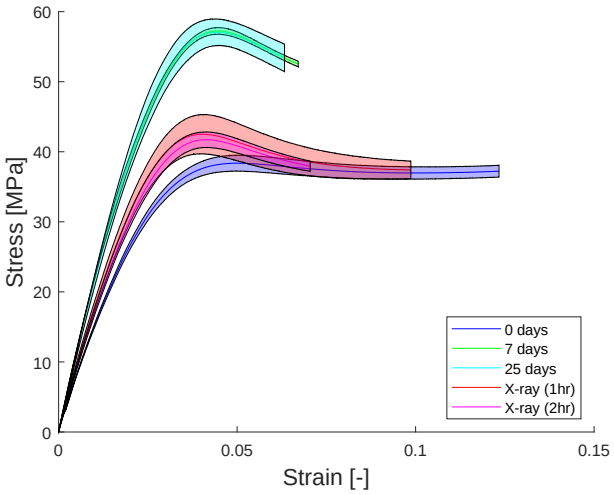

Figure 6. Quasi-static tensile: stress-strain diagram.

3.2. Quasi-static and dynamic compressive loading

The stress-strain diagrams were created from the measured compressive test data. The individual average aging curves were again compared with each other and from the resulting stress-strain diagrams (see Figure 7) similar trends to those for tensile loading can be observed. The curves corresponding to the samples exposed to solar radiation have similar trends, showing a steeper increase in the elastic strain region, and higher strengthening. Samples tested after 25 days have slightly higher values than samples tested after 7 days. The specimens tested immediately after manufacture show the highest resistance to failure. An important difference with tensile loading is the order of magnitude higher values achieved for compressive loading.

When comparing quasi-static and dynamic compressive loading (see Figure 8), significant differences in the loading behaviour of the specimens can be observed. The curves show different trends – the spec-

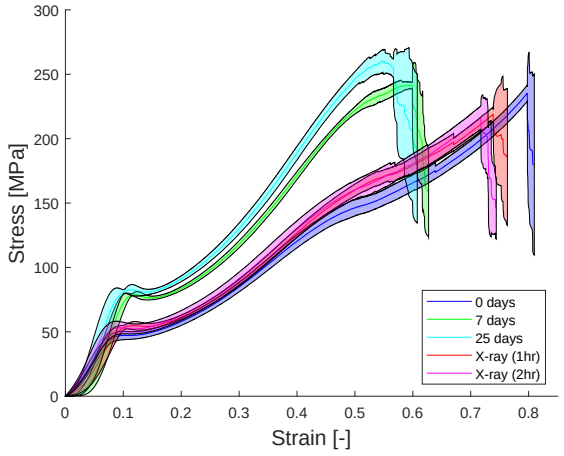

FIGURE 7. Quasi-static compressive: stress-strain diagram.

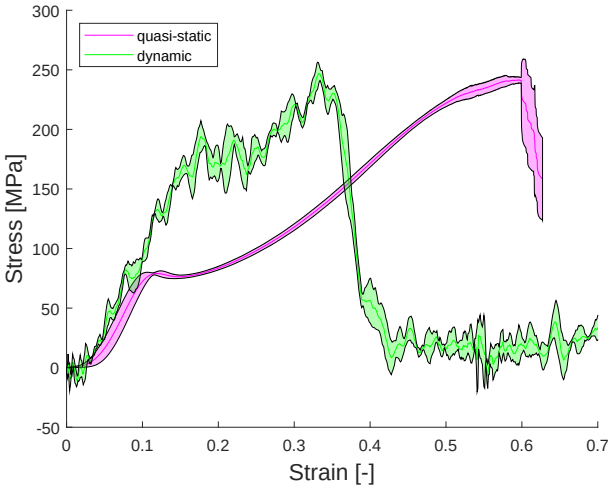

FIGURE 8. Comparison of quasi-static and dynamic compressive loading.

imens tested by dynamic compressive test show up to twice as much strengthening and failure occurs much earlier (sudden rapid drop in stress in the diagram) than the specimens tested by quasi-static test. In contrast, the area of plastic deformation of these specimens is quite extensive.

4. CONCLUSIONS

Using additive manufacturing called Stereolithography, two types of 3D printed test specimens were produced – for tensile and compressive testing. Subsequently, these samples were exposed to two types of aging – sunlight and extreme X-ray for varying lengths of time. These specimens were subjected to 3 loading tests: quasi-static tensile loading, quasi-static compressive loading, dynamic compressive loading. From the measured data, the basic mechanical parameters were calculated and stress-strain diagrams were plotted. From these, it was possible to observe the acquisition of different values of the basic mechanical parameters and differences in the individual trends of the curves in the diagram depending on the type of aging and the time of exposure. The samples exposed to solar radiation generally reached higher values than the remaining samples, but at the same time they showed earlier failure. Other major differences were shown by comparing quasi-static and dynamic compressive loading, where dynamic loading resulted in a significant strengthening of the material during loading.

Based on the data obtained, it was shown that the aging process causes significant changes in the mechanical properties of the materials used, which could have a consequential impact on their use in different industries.

ACKNOWLEDGEMENTS

There is very appreciated a kind sponsorship of grants from Czech Science Foundation – Junior Star (project no. 22-18033M) and CTU internal project SGS22/196/OHK2/3T/16.

REFERENCES

[1] C. Parulski, O. Jennotte, A. Lechanteur, B. Evrard. Challenges of fused deposition modeling 3D printing in pharmaceutical applications: Where are we now? *Advanced Drug Delivery Reviews* **175**:113810, 2021. https://doi.org/10.1016/j.addr.2021.05.020

[2] Z. Weng, Y. Zhou, W. Lin, et al. Structure-property relationship of nano enhanced stereolithography resin for desktop SLA 3D printer. *Composites Part A: Applied Science and Manufacturing* **88**:234–242, 2016. https://doi.org/10.1016/j.compositesa.2016.05.035

[3] H. Agrawaal, J. Thompson. Additive manufacturing (3D printing) for analytical chemistry. *Talanta Open* **3**:100036, 2021. https://doi.org/10.1016/j.talo.2021.100036

[4] K. G. Topsakal, M. Aksoy, G. S. Duran. The effect of aging on the mechanical properties of 3-dimensional printed biocompatible resin materials used in dental applications: An in-vitro study. *American Journal of Orthodontics and Dentofacial Orthopedics* **164**(3):441–449, 2023. https://doi.org/10.1016/j.ajodo.2023.05.023

[5] N. Mite-Guzmán, M. Lazo, J. Triguero, et al. Two-dimensional infrared for monitoring the structural variations of UV-aged recycled polypropylene straps used in the ecuadorian banana industry. *Case Studies in Chemical and Environmental Engineering* **7**:100359, 2023. https://doi.org/10.1016/j.cscee.2023.100359

[6] V. Drechslerová, M. Neuhäuserová, J. Falta, et al. Stereolithography for manufacturing of advanced porous solids. *Acta Polytechnica CTU Proceedings* **41**:1–7, 2023. https://doi.org/10.14311/APP.2023.41.0001

[7] Phrozen. Phrozen Aqua Blue, 2020. [2023-08-04], https://c-3d.niceshops.com/upload/file/MSDS_English-Phrozen_Aqua_Blue.pdf.

[8] J. Šleichrt, T. Fíla, P. Koudelka, et al. Dynamic penetration of cellular solids: Experimental investigation using Hopkinson bar and computed tomography. *Materials Science and Engineering: A* **800**:140096, 2021. https://doi.org/10.1016/j.msea.2020.140096